Published in final edited form as:
Nat Med. 2017 September ; 23(9): 1046–1054. doi:10.1038/nm.4372.

Opposing effects of cancer type-specific SPOP mutations on BET protein degradation and sensitivity to BET inhibitors

Hana Janouskova[#1,2], **Geniver El Tekle**[#1,2,3], **Elisa Bellini**[4], **Namrata D. Udeshi**[5], **Anna Rinaldi**[1,2], **Anna Ulbricht**[6], **Tiziano Bernasocchi**[1,2,3], **Gianluca Civenni**[1,2], **Marco Losa**[1,2], **Tanya Svinkina**[5], **Craig M. Bielski**[5,§], **Gregory V. Kryukov**[5], **Luciano Cascione**[1,2], **Sara Napoli**[1,2], **Radoslav I. Enchev**[6], **David G. Mutch**[7], **Michael E. Carney**[8], **Andrew Berchuck**[9], **Boris J.N. Winterhoff**[10], **Russell R. Broaddus**[11], **Peter Schraml**[4], **Holger Moch**[4], **Francesco Bertoni**[1,2], **Carlo V. Catapano**[1,2,3], **Matthias Peter**[6], **Steven A. Carr**[5], **Levi A. Garraway**[5,12,13], **Peter J. Wild**[4], and **Jean-Philippe P. Theurillat**[1,2,3,+]

[1]Institute of Oncology Research, Oncology Institute of Southern Switzerland, Bellinzona, TI 6500, Switzerland [2]Faculty of Biomedical Science, Università della Svizzera Italiana, Lugano, CH 6904, Switzerland [3]Centre Hospitalier Universitaire Vaudois, University of Lausanne, Lausanne, VD 1011, Switzerland [4]Institute of Surgical Pathology, University Hospital Zurich, Zurich, ZH 8091, Switzerland [5]The Broad Institute of Harvard and MIT, Cambridge, MA 02142, USA [6]Department of Biochemistry, Eidgenössische Technische Hochschule, Zurich, Switzerland [7]Division of Gynecologic Oncology, The Washington University, St. Louis, MO, 63130, USA [8]Department of Obstetrics Gynecology and Women's Health, University of Hawaii Cancer Center, HI 96813, USA [9]Division of Gynecologic Oncology, Duke Cancer Center, Durham, NC 27710, USA [10]Division of Gynecologic Oncology, University of Minnesota, Minneapolis, MN 55455, USA [11]Department of Pathology, the University of Texas MD Anderson Cancer Center, Houston, TX 77030, USA [12]Department of Medical Oncology, Dana-Farber Cancer Institute, Boston, MA 02115, USA [13]Center for Cancer Genome Discovery, Dana-Farber Cancer Institute, Boston, MA 02115, USA

[+]Correspondence and requests for materials should be addressed to J.P.T. (jean-philippe.theurillat@ior.iosi.ch).
[§]Current address: Molecular Oncology, Memorial Sloan Kettering Cancer Center, New York, USA

Author Contributions

J.-P.P.T. originally developed the concept, further elaborated on it and designed the experiments together with H.J., G.E.T., N.D.U. H.J., G.E.T., A.R., J.-P.P.T., N.D.U., T.S., S.N., A.U., R.I.E. performed experiments and analysed the data.. H.J., G.C., G.E.T. and T.B. performed xenograft tumor experiments in immune-deficient mice. M.L., H.J. and J.-P.P.T. performed immunohistochemical experiments and analysis. P.J.W., P.S., H.M. and E.B. provided endometrial and prostate cancer samples with annotated for *SPOP* mutation status. D.G.M., M.E.C., A.B., B.J.N.W. and R.R.B. provided SPOP-mutant endometrial cancer samples. C.M.B., G.V.K., A.R., and L.C. analyzed genomic and RNAseq data. J.-P.P.T., L.A.G., S.A.C., M.P., C.V.C., F.B., P.J.W. provided funding and resources. J.-P.P.T., H.J. and G.E.T. interpreted the data and wrote the paper. H.J. and G.E.T. contributed equally to this work.

Competing Financial Interest

L.A.G is a paid consultant of the following pharmaceutical companies: Novartis Foundation Medicine, Boehringer INgelheim, and Millennium/Takeda. The authors declare no additional competing financial interests.

Data Availability

Cancer cell line encyclopedia data is online available under http://www.broadinstitute.org/ccle/home. The original mass spectra have been deposited in the public proteomics repository MassIVE and are accessible at ftp://MSV000080401@massive.ucsd.edu when providing the dataset password: ubiquitin. If requested, also provide the username: MSV000080401. Sequencing data have been deposited in the NCBI public database and are accessible at https://www.ncbi.nlm.nih.gov/bioproject/PRJNA357942. These data will be made public upon acceptance of the manuscript. Reprints and permissions information is available at www.nature.com/reprints.

Europe PMC Funders Author Manuscripts

[#] These authors contributed equally to this work.

Abstract

It is generally assumed that recurrent mutations within a given cancer driver gene elicit similar drug responses. Cancer genome studies have identified recurrent but divergent missense mutations in the substrate recognition domain of the ubiquitin ligase adaptor SPOP in endometrial and prostate cancer. Their therapeutic implications remain incompletely understood. Here, we analyzed changes in the ubiquitin landscape induced by endometrial cancer-associated *SPOP* mutations and identified BRD2, BRD3 and BRD4 proteins (BETs) as SPOP-CUL3 substrates that are preferentially degraded by endometrial SPOP mutants. The resulting reduction of BET protein levels sensitized cancer cells to BET inhibitors. Conversely, prostate cancer-specific SPOP mutants impaired degradation of BETs, promoting resistance against their pharmacologic inhibition. These results uncover an oncogenomics paradox, whereby mutations within the same domain evoke opposing drug susceptibilities. Specifically, we provide a molecular rationale for the use of BET inhibitors to treat endometrial but not prostate cancer patients with *SPOP* mutations.

Specific cancer gene mutations can indicate whether a cancer patient may or may not respond to a given drug1. Generally, it is assumed that recurrent mutations within a specific gene have similar therapeutic implications, especially, if the amino acid changes occur within the same protein-encoding domain. Genome studies have revealed recurrent point mutations within the substrate recognition domain of the encoding ubiquitin ligase adaptor speckle-type POZ protein (SPOP) in 4-14% of prostate and endometrial cancers (Fig. 1a)2–6. In prostate cancer, SPOP mutations are confined to amino acid residues of the substrate-binding cleft - a specific region within the substrate-recognition domain that is essential for substrate interaction and ubiquitin transfer7. We and others have subsequently shown that these mutations act in a dominant-negative fashion to repress ubiquitylation and degradation of oncogenic substrate proteins8–12. In contrast, recurrent amino acid substitutions in endometrial cancer and carcinosarcoma occur in an uncharacterized territory of the substrate recognition domain (Fig. 1a and Supplementary Fig. 1a)4–6. Given the divergent mutation pattern in these tumor types, we speculated that endometrial cancer SPOP mutations might differently affect protein ubiquitylation, possibly resulting in distinct therapeutic opportunities.

Results

Cancer type-specific SPOP mutations have opposing effects on BET protein levels

To explore this hypothesis, we characterized the changes in the ubiquitination landscape specific to endometrial cancer SPOP mutations by mass-spectrometry-based proteomics. To ensure that disease relevant proteins are being expressed in our experimental setting, we chose human Ishikawa endometrial cancer cells, derived from a well-differentiated endometrioid cancer, because their robustly expressed genes significantly overlayed with those found in *SPOP*-mutant tumor tissues (Supplementary Fig. 1b)6,13. Subsequently, we stably overexpressed control vector (control); SPOP wild-type (SPOP-WT); or seven mutated SPOP variants (SPOP-E47K, -E50K, -E78K, -S80R, -M117V, -R121Q, -D140N (SPOP-MTs) (Supplementary Fig. 1c) in these cells. In each case, we measured glycine-

glycine remnants of ubiquitylated lysines (K-ε-GG) after trypsin digestion and stable isotope labeling of amino acids in cell culture (SILAC)–based mass-spectrometry (LC-MS/MS) (Supplementary Fig. 1d)14. All K-ε-GG values (n = 17 239) were normalized to protein abundance to account for ubiquitylation-related changes in protein expression (Supplementary Table 1). K-ε-GG-peptide values of individual SPOP-MTs were compared to cells overexpressing SPOP-WT within experiments (Supplementary Fig. 2a,c,e,g).

Because protein ubiquitylation is often linked to proteasomal degradation, we asked which differentially expressed K-ε-GG peptides showed an inverse correlation with protein expression (Supplementary Table 1 and Supplementary Fig. 2b,d,f,h). Thereby, we identified two patterns of ubiquitination and protein dysregulation in known and putative SPOP substrates pointing to possible private contact points between individual substrates and the mutant MATH domain (Fig. 1b,c and Supplementary Figs. 2,3a). Peptides corresponding to TRIM24, AGR2, and NCOA3 – all proteins with reported oncogenic properties - showed a decrease in K-ε-GG abundance followed by a raise in corresponding protein levels9,15,16. Similar dominant-negative patterns of substrate dysregulation have been reported for TRIM24 and NCOA3 by prostate cancer SPOP mutations8,9,17.

The most striking changes were found in proteins that exhibited a robust up-regulation of K-ε-GG peptides coupled with down-regulation of the corresponding protein (Fig. 1b,c and Supplementary Fig. 2,3a), including DEK, another characterized SPOP substrate8. Yet, the most profound protein changes without concurrent changes at the mRNA level were found in BRD3, BRD2, and BRD4 (Fig. 1b,c and Supplementary Fig. 3b). These bromodomain and extra-terminal (BET) motif containing proteins, which serve as promising targets for cancer therapy18, may be increasingly ubiquitylated and degraded by endometrial cancer SPOP mutants. Importantly, similar changes were found also in human HEC-151 and RL-952 endometrial cancer cells, and in human 22Rv1 prostate cancer cells (Supplementary Fig. 3c-e).

Because prostate cancer SPOP mutants have been found to impair ubiquitylation of substrates in a dominant-negative manner, we speculated that these mutants might have an opposite effect on BET protein levels8–11. Indeed, over-expression of recurrent prostate cancer mutants increased BET protein levels in human Ishikawa endometrial cancer cells, human 22Rv1 prostate cancer, human LHMAR prostate epithelial cells8 (Fig. 1d,e and Supplementary Fig. 3f-h) and in mouse prostate epithelial cells19. In aggregate, our findings suggest that BET proteins might represent SPOP substrates that become differentially ubiquitylated and degraded by endometrial and prostate cancer mutants irrespective of cellular lineage. In support, nuclear levels of BET proteins correlated inversely with recurrent *SPOP* mutations in human primary endometrial cancer tissues analyzed by immunohistochemistry, whereas a positive correlation in human primary prostate cancer tissues was noted (Fig. 1f,g and Supplementary Fig. 4).

BET proteins are *bona fide* SPOP substrates

We sought to determine whether SPOP directly interacts with BET proteins to promote ubiquitylation. In agreement, the primary amino acid sequence of BET proteins contained a conserved consensus of SPOP-binding motif (Fig. 2a)7. We focused on BRD3 for

experimental follow up, because it was the most differentially regulated BET family member (Fig. 1b). First, we overexpressed HA-tagged BRD3 harboring three threonine-to-alanine substitutions at the binding motif (Degron-MT) (Supplementary Fig. 5a) and assessed the ability of SPOP-WT to mediate BRD3 degradation. Indeed, the degron-variant abolished the repressive effect of SPOP and produced elevated levels of BRD3 protein, in agreement with the notion that also endogenous SPOP was not able to degrade the degron-variant (Fig. 2b and Supplementary Fig. 5b). To determine whether this motif mediated direct binding of SPOP to BRD3, we performed immunoprecipitation experiments in cells expressing either wild-type HA-BRD3 or the degron variant. Whereas SPOP protein was detectable after immunoprecipitation of HA-BRD3, the BRD3 degron variant disrupted the BRD3-SPOP interaction (Fig. 2c). Thus, the SPOP-binding motif within BRD3 appeared necessary for SPOP binding.

Next, we tested whether SPOP could ubiquitylate BRD3 as part of a CUL3-RBX1 ubiquitin E3 ligase complex20. Knockdown of *CUL3* increased HA-BRD3 levels and decreased BRD3 ubiquitylation (Supplementary Fig. 5c). Furthermore, SPOP-WT along with RBX1 and CUL3 directly ubiquitylated HA-BRD3 *in vivo* and *in vitro*, whereas the degron variant of HA-BRD3 remained unaffected (Fig. 2d and Supplementary Fig. 5d). Additional CUL3-dependent substrate adaptors (KLHL9, KLHL13, KLHL21) failed to ubiquitylate BRD3 *in vitro* and thus verified the specificity of SPOP towards BRD3 (Supplementary Fig. 5d).

To determine if BRD3 ubiquitylation induces its proteasomal degradation, we cultured SPOP- and BRD3-expressing cells in the presence or absence of the proteasome inhibitor MG132. Short-term MG132 treatment increased ubiquitylated HA-BRD3 (Fig. 2d). Prolonged proteasomal inhibition, increased HA-BRD3 and endogenous BET protein levels in the presence of SPOP-WT overexpression (Fig. 2e and Supplementary Fig. 5e). SPOP protein was also detectable after immunoprecipitation of endogenous BET proteins (Supplementary Fig. 5f). Moreover, *SPOP* knockdown increased BET protein levels without concomitant mRNA changes and impaired protein degradation after inhibition of protein synthesis with cycloheximide (Fig. 2f and Supplementary Fig. 5g, h). In aggregate, these data are consistent with a model in which ubiquitylation of BET proteins promote their proteasomal degradation.

Cancer type-specific SPOP mutants induce differential ubiquitylation of BET proteins

To test if the functional properties of endometrial cancer SPOP mutants may translate into reduced BET protein levels when expressed at the endogenous level, we identified in the Cancer Cell Line Encyclopedia the human endometrial cancer cell line EN that harbors a recurrent SPOP-R121Q mutation (Supplementary Fig. 6a). We compared BET protein levels of EN cells to Ishikawa cells with equal levels of wild type SPOP (Fig. 3a). Indeed, EN cancer cells exhibited lower levels of BET proteins, despite higher levels of corresponding mRNAs (Fig. 3a and Supplementary Fig. 6b). In line with the notion that enhanced protein degradation by SPOP-R121Q reduced BET protein levels in EN cells, we found more significant increases of BET protein levels upon SPOP depletion or short-term proteasome inhibition in EN cells compared to Ishikawa cells (Fig. 3b and Supplementary Fig. 6c-e). In addition and consistent with our observations above, endogenous SPOP-R121Q bound more

efficiently to BET proteins in EN cells in which we noted a more pronounced degradation of BET proteins after inhibition of protein synthesis with cycloheximide (Fig. 3c and Supplementary Fig. 6f,g). Of note, endogenous SPOP levels were also increased after prolonged proteasome inhibition and reduced after inhibition of protein synthesis, indicating a proteasomal turnover of SPOP itself (Fig. 2e and Fig. 3b,c).

To test if altered BET protein binding and degradation kinetics in human EN and Ishikawa cells were a result of specific amino acid substitutions within SPOP, we analyzed the effects of different SPOP species side-by-side in the same cellular context. Endometrial cancer SPOP-E50K and SPOP-R121Q mutants bound more strongly to HA-BRD3 than SPOP-WT *in vivo* and *in vitro*, whereas the interaction was reduced with the prostate cancer SPOP-W131G and SPOP-F133L mutants, respectively (Fig. 3d and Supplementary Fig. 6h). In line, ubiquitylation of HA-BRD3 was increased by the endometrial cancer and decreased by prostate cancer SPOP mutants, respectively (Fig. 3e and Supplementary Fig. 6i). We next investigated if the increase in ubiquitylation mediated by the endometrial cancer SPOP mutants is dependent on the intact degron on BRD3. Indeed, SPOP-E50K failed to ubiquitylate the degron variant of BRD3 (Fig. 3f) and to reduce its protein levels (Supplementary Fig. 6j). These results suggest that BET protein levels are at least in part affected by differential interaction between SPOP mutants and the BET degron.

Sensitivity to BET inhibitors is altered by cancer type-specific SPOP mutants

Some cancer cells typically depend on the presence of BET proteins for tumor growth and survival18,21. Therefore, we wondered whether enhanced degradation of BET proteins in the context of endometrial cancer SPOP mutant might create specific vulnerabilities. We speculated that endometrial cancer cells with low BET protein levels might become particularly susceptible to further reduction of BET proteins. Indeed, the growth of EN cells were susceptible to single knockdown of BET proteins (Supplementary Fig. 7a). To achieve a similar effect in Ishikawa cells, individual BET proteins had to be knocked down in the context of SPOP-R121Q over-expression, in analogy to EN cells. These data suggest that endometrial cancer cells with low BET protein levels in the context of endometrial cancer SPOP mutant are particularly susceptible to further suppression of BET protein function. In support of this view, a functional overlap among BET proteins has been reported22.

BET inhibitors are under clinical investigation as anti-cancer therapeutics, including solid tumors18,21,23,24. We anticipated that the susceptibility of cancer cells to these inhibitors might be influenced by BET protein level changes in response to SPOP mutants. Indeed, forced expression of endometrial cancer SPOP mutants (shown previously to lower BET protein levels) sensitized Ishikawa cells to both BET inhibitors JQ1 and OTX-015 by promoting apoptosis and reducing cellular proliferation (Fig. 4a and Supplementary Fig. 7b-e)25,26. Similar results were also found in HEC151 and RL952 endometrial cancer cells (Supplementary Fig. 7f). We wondered whether BET protein level changes contribute to JQ1 sensitivity. To this end, reduced level of the individual BET proteins in response to SPOP mutants in Ishikawa cells correlated with the decrease of the half maximal inhibitory concentration (IC_{50}) after JQ1 treatment (Fig. 4b). Functionally, overexpression of BRD2, BRD3, and BRD4 degron variants lowered SPOP-E50K-mediated JQ1 sensitization (Fig. 4c

and Supplementary Fig. 7g). We then investigated whether increased BET protein levels in the context of prostate cancer may on the contrary induce resistance to BET inhibitors. Overexpression of prostate cancer SPOP mutants rendered Ishikawa cells and 22Rv1 more resistant to JQ1 (Fig. 4a and Supplementary Fig. 7h,i), while individual (Fig. 4d and Supplementary Fig. 7j,l) or combined knockdown (Supplementary Fig. 7k) of BET proteins in the context of SPOP-Y87C mutant dampened this phenotype.

Next, we wondered if recurrent SPOP mutations or decreased BET protein levels in general may predict sensitivity to pharmacological BET inhibition across human endometrial cancer cell line models. For this purpose, we assessed JQ1-sensitivity in 3D semi-solid culture conditions across 12 different human cell lines for which we determined BET protein levels in parallel. Decreased expression levels of BRD2, BRD3, and BRD4 was associated in many cases with sensitivity to JQ1 (Supplementary Fig. 8a-c), however we noted also some remarkable exceptions to this rule in agreement with the existence of other molecular mechanisms that regulate BET inhibitor susceptibility27,28. Nevertheless, SPOP-R121Q-mutant EN cells were sensitive to JQ1 inhibition in line with our previous data generated in isogenic cell lines (Fig. 4a,e and Supplementary Fig. 7f, 8b). This finding let us to search for additional cell lines with recurrent endometrial cancer-associated *SPOP* mutations at the endogenous locus. We identified in the Cosmic Cell Line Project a colorectal and a urothelial cancer cell line that harbor a SPOP-E47K (NCI-H508) and SPOP-E50K (VM-CUB1) mutation, respectively. Both cell lines were particularly sensitivity to JQ1 and displayed low BET protein levels that were responsive to proteasomal inhibition (Fig. 4e and Supplementary Fig. 8d). Thus, endometrial cancer-associated *SPOP* mutations may possibly be more broadly associated with BET inhibitor sensitivity.

Moreover, we tested if established SPOP substrates may influence either directly or indirectly JQ1 responses through changes in BET proteins levels. Neither knockdown nor overexpression of DEK, TRIM24, NCOA3, nor ERG lead to significant changes of BET protein levels or JQ1 responses, further supporting the notion that SPOP mutants affect JQ1 sensitivity directly through regulation of BET protein degradation (Supplementary Fig. 9).

Transcriptome analysis identifies *FOSL1* as determinant of JQ1 response

BET inhibitors bind to the bromodomains of BET proteins to displace them from acetylated histone tails of transcriptionally active sites. Given this function, we interrogated the transcriptional changes in response to over-expression of wild type SPOP or two recurrent endometrial and prostate cancer SPOP mutants in Ishikawa cells (Supplementary Table 2). Unsupervised clustering and multidimensional scaling (MDS) analysis revealed mainly opposing changes of endometrial and prostate cancer SPOP mutants, whereby wild type SPOP positioned in between the different types of SPOP mutants (Supplementary Fig. 10a-b). This result aligns well with the BET protein level changes across the different cell lines observed earlier (Supplementary Fig. 3f). Interestingly, the MDS analysis revealed a second feature that discriminated both types of mutants from wild type SPOP, possibly reflecting shared dysregulation of SPOP substrates such as TRIM24 or NCOA3 (Fig. 1c and Supplementary Fig. 10b)8.

Next, we interrogated the transcriptional changes under JQ1 treatment in endometrial versus prostate cancer SPOP mutants and found a significant overlap with the genes altered in the untreated conditions (Fig. 5a,b and Supplementary Fig. 10a-c). We identified 16 genes that were shared across all conditions (untreated, 500 nM and 2 μM JQ1 treated) including *FOSL1* – a reported BET protein target gene implicated in BET inhibitor sensitivity29. FOSL1 mRNA and protein expression was reduced in endometrial compared to prostate cancer SPOP mutants, consistent with the BET protein level changes and the transcriptome analysis (Fig. 5c). Importantly, in human tumor tissues FOSL1 mRNA and protein expression was also decreased in SPOP-mutant endometrial cancer patients, whereby the lowest mRNA levels were observed in patients that harbored SPOP mutants shown to have in our study the strongest effects on BET protein levels and JQ1-sensitivity (Fig. 5 d,e and Supplementary Fig. 7c)30–33.

Next, we asked whether BET protein level changes in response to SPOP mutants and JQ1 may decrease *FOSL1* transcription. To this end, a triple occupancy of BRD2, BRD3, and BRD4 has been reported at the *FOSL1* promoter (Supplementary Fig. 10d)24. JQ1 treatment reduced FOSL1 expression levels in all conditions, while preserving the differences between the different types of SPOP mutants (Fig. 5f). Knockdown of individual *BET* proteins decreased *FOSL1* transcription in JQ1-resistant Ishikawa cells over-expressing the prostate cancer SPOP-Y87C variant (Fig. 4a and Supplementary Fig. 10e). Moreover, *FOSL1* depletion itself directly lowered JQ1 resistance in this setting, indicating a functional involvement of this gene downstream of BET protein changes and SPOP mutants (Fig. 5g). Taken together, these results suggest that BET protein level changes in response to SPOP mutants alter at least in part JQ1 susceptibility through transcriptional regulation of *FOSL1*.

JQ1 treatment blocks tumor growth in endometrial SPOP mutant xenografts *in vivo*

Finally, we investigated whether our results on altered JQ1 sensitivity in response to SPOP mutants were validated in an *in vivo* setting. For this purpose, we focused on endometrial cancer-associated SPOP mutants because this setting may identify patients with particular beneficial responses to BET inhibitors. Indeed, JQ1 efficiently blocked the growth of xenograft tumor models established from SPOP-mutant EN cells by reducing cell proliferation and inducing apoptosis, whereas Ishikawa-derived tumors were largely resistant to JQ1 treatment (Fig. 6a-c). Consistent with *in vitro* data, forced expression of SPOP-E50K or SPOP-S80R sensitized Ishikawa cells to JQ1 *in vivo* (Fig. 6d,e).

Discussion

Recurrent missense mutations in *SPOP* – encoding a substrate receptor of a cullin-RING ubiquitin ligase - have emerged in 5-10 % of comprehensive prostate and endometrial cancer genome sequencing studies2–6. Surprisingly, the specific genetic alterations show no overlap between the tumor types, even though they are confined to the same substrate recognition domain. While the prostate cancer-associated mutations have been more recently shown to stablize protein substrates relevant to prostate tumorigenesis9–12,34, the therapeutic implication of both mutation types remain largely elusive.

Our study identifies the BET proteins (BRD2, BRD3, and BRD4) as *bona fide* SPOP substrates. Small-molecule inhibitors against this group of proteins are under clinical investigation in hematological and solid tumors because of their critical importance in driving lineage-specific oncogenic transcriptional programs18,21,23,24. We found that prostate cancer-associated SPOP mutations impair degradation of BET proteins in line with their loss-of-function properties reported previously8,9, while endometrial cancer-associated SPOP mutations enhance BET proteins degradation through a gain-of-function mechanism (Fig. 6f). The precise structural basis on how endometrial SPOP mutants enhance binding and ubiquitylation of BET proteins and other substrates (e.g. DEK) remains to be further elucidated. The altered BET protein levels in the SPOP mutant setting influence the transcription of established target genes such as *FOSL1*29 and thereby alter the susceptibility of cancer cells to BET inhibitors. Of note in this regard, a recent report implies enhanced FOSL1 activity as a mechanism of acquired resistance in ovarian cancer cells as well35. Overall, our established model extends the list of previously reported mechanisms that influence BET inhibitor sensitivity27,36,37 .

BET inhibitors are currently under clinical development and there is a critical need to identify patients that may respond to the treatment. Our preclinical study identifies SPOP mutations as a clinically detectable biomarker of BET inhibitor response. Thus, the detection of specific *SPOP* mutations may be used to select patients that may (endometrial cancer-associated *SPOP* mutations) or may not (prostate cancer-associated *SPOP* mutations) benefit from the BET inhibitors treatment.

More generally, our results suggest a paradigm whereby mutations within the same domain of a particular protein evoke opposing drug susceptibilities. Given the increasing use of cancer genome information in a clinical setting, caution may be applied to extrapolate therapeutic responses based on similar mutations.

Methods

SILAC-labeling and Cell Culture

For SILAC experiments, human endometrial cancer cells Ishikawa were cultured in DMEM/F12 media deficient in L-arginine and L-lysine and supplemented with 10% dialyzed fetal bovine serum (FBS) (Sigma-Aldrich), penicillin, streptomycin, and L-glutamine (Invitrogen) and either L-arginine (Arg-0) and L-lysine (Lys-0), L-arginine [$^{13}C_6$]HCl (Arg-6) and L-lysine-4,4,5,5-d4 (Lys-4), or [$^{13}C_6$, $^{15}N_4$]HCl (Arg-10) and L-lysine [$^{13}C_6$,$^{15}N_2$]HCl (Lys-8) (Sigma-Aldrich) for 14 days (10 doublings). All media were supplemented with L-proline to prevent the conversion of arginine to proline38. Specifically, isogenic cell lines expressing either vector control (C), wild type SPOP (SPOP-WT) or mutants (MTs) were isotopically labeled with SILAC media and grouped into four experiments (Supplementary Fig. 1d). Each experiment included a cell line with over-expression of SPOP-WT for cell line comparison within and across experiments. The labeling for this cell line was switched to rule out labeling artifacts in the first three experiments. Approximately 100 million cells per condition were washed twice with PBS, harvested, and snap frozen.

Europe PMC Funders Author Manuscripts

K-ε-GG profiling and proteome analysis by liquid chromatography mass-spectrometry

Preparation of proteins for mass spectrometry analysis was completed as previously described14. Briefly, cell pellets were lysed in an ice cold urea lysis buffer containing, 8 M urea, 50 mM Tris HCl, pH 8, 150 mM NaCl, 1 mM EDTA, 2 ug/ml aprotinin (Sigma-Aldrich), 10 mg/ml leupeptin (Roche Applied Science), 1 mM phenylmethylsulfonyl fluoride (PMSF), 50 uM PR-619, and 1 mM chloroacetamide. The lysate was cleared by centrifugation at 20,000*g* for 10min. A bicinchoninic acid (BCA) protein assay (Thermo Fisher Scientific) was used to determine the protein concentration of each sample. Respective SILAC mixes were created by combining equal amount of protein per SILAC state. Proteins were reduced with 5 mM DTT at RT and subsequently alkylated with 10 mM iodoacetamide at RT in the dark. Lysates were diluted 1:4 with 50 mM Tris HCl, pH 8 and proteins were digested with sequencing grade trypsin using an enzyme to substrate ratio of 1:50, O/N at 25 C. Digests were quenched with TFA and the peptide solutions were cleared by centrifugation prior to desalting. Peptides were desalted using tC18 SepPak SPE cartridges (Waters) exactly as previously described14.

Peptides were fractionated offline by basic pH reversed-phase (bRP) chromatography as previously described14,39. Input for each bRP separation was equivalent to 30 mg of starting protein material (10 mg protein per SILAC state) for replicate. Briefly, dried peptides were reconstituted in bRP buffer A (5 mM ammonium formate (pH 10.0)/2% acetonitrile). A Zorbax 300 Extend-C18 column (9.4 × 250 mm, 300 Å, 5 μm; Agilent) was used for the separation. Using the gradient and flow rate settings previously described14 a total of 96 2 ml fractions were collected across the entirety of the bRP separation. For proteome analysis, 5% of each fraction was taken and combined in a non-contiguous manner such that every 24th fraction was combined to create 24 final fractions. For K-ε-GG analysis, the remainder of each fraction was combined in a non-contiguous manner such that every eighth fraction was combined to create 8 final fractions. Pooled fractions were dried completely using vacuum centrifugation.

For enrichment of K-ε-GG peptides, anti-K-ε-GG antibody from the PTMScan ubiquitin remnant motif (K-ε-GG) kit was utilized (Cell Signaling Technology, cat. no. 5562). Prior to enrichment, the antibody was cross-linked to protein A beads using dimethyl pimelimidate (DMP)14. Peptides were reconstituted in immunoaffinity purification (IAP) buffer and the enrichment was completed exactly as previously described14. Briefly, peptides were incubated with approximately 31 ug of anti-K-ε-GG antibody beads and incubated for 1 h at 4 °C with rotation. Beads were washed twice with 1.5 ml of ice-cold IAP buffer followed by three washes with ice-cold PBS. K-ε-GG peptides were eluted from the antibody with 2 x 50 ul of 0.15% TFA. Peptides were desalted using StageTips. StageTips were conditioned by washing with 50 ul of 50 % MeCN/0.1% formic acid (FA) followed by 2 x 50 ul of 0.1% FA. Peptides were then loaded on StageTips, washed 2 x with 50 ul of 0.1% FA and eluted with 50 ul of 50 % MeCN/0.1% formic acid (FA). Eluted peptides were dried completely using vacuum centrifugation.

Samples were reconstituted in 3% MeCN/0.1% FA. All samples were analyzed by nanoflow-UPLC-HCD-MS/MS using a Q Exactive mass spectrometer (Thermo Fisher Scientific) coupled online to an Easy-nLC 1000 system (Proxeon). For K-ε-GG and

proteome samples, 4/8 ul and 1/20 ul were injected into the mass spectrometer, respectively. Samples were injected at a flow rate of 500 nl/min onto a PicoFrit column (360 μm (OD) × 75 μm (ID), 10 μm ID tip, 50 cm length (New Objective) self-packed with 24 cm of ReproSil-Pur 120 Å, 1.9 μm C18-AQ beads. The nanoflow column was heated to 50 °C using a column heater (Pheonix S&T). For LC-MS/MS analyses, the gradient and flow rate settings were used as previously described14 and the MS acquisition time used for each K-ε-GG and proteome sample was 120 min. The Q Exactive was operated by acquiring an MS1 scan (R=70,000) followed by MS/MS scans (R=17,500) on the 12 most abundant ions. An MS1 and MS2 ion target of 3 x 10^6 and 5 x 10^4 ions, respectively was used for acquisition. A maximum ion time of 10 ms and 120 ms was used for MS1 and MS2 scans, respectively. The isolation width was set to 2.5 m/z, the HCD collision energy was set to 25, the dynamic exclusion time was set to 20 s,and the peptide match and isotope exclusion functions were enabled. A second round of bRP fractionation, K-ε-GG, and MS analysis was completed for experiment 3 and 4 (6 mg per SILAC state for experiment 3 and 10 mg per SILAC state replicate 4).

MS Data Analysis

Data were processed using the MaxQuant (version 1.2.2.5) software package. The human Uniprot database including 248 common laboratory contaminants was used for searching. The enzyme specificity was set to trypsin, the maximum number of missed cleavages was set to 2 for proteome data and 4 for K-ε-GG data , the precursor mass tolerance was set to 20 ppm for the first search, and the tolerance was set to 6 ppm for the main search. Carbamidomethylation of cysteines was searched as a fixed modification and oxidation of methionines and N terminal acetylation of proteins was searched as variable modifications.

For K-ε-GG data, addition of glycine-glycine to lysine was also searched as a variable modification. For identification, the minimum peptide length was set to 7, and the false discovery rate for peptide, protein, and side identification was set to 1 %. The filter labeled amino acids and peptide quantification functions were enabled. For proteome data, normalized ratios were obtained from the ”proteinGroups” table. For K-ε-GG data, normalized SILAC ratios were obtained from the ”GlyGly(K)Sites” table.

For K-ε-GG and proteome datasets, reverse and contaminant hits were removed from the analysis. Proteins were considered in the dataset if they were identified and quantified by 2 or more razor/unique peptides in each SILAC triple-labeled experiment. K-ε-GG peptides were considered for the final dataset if the corresponding protein was quantified in the proteome data.

To capture ubiquitylation changes associated with protein degradation, we normalized the K-ε-GG changes to their measured protein levels. The leading accesion number was used to match the protein and K-ε-GG data. Quantitative, protein-normalized measurements were available for 17,239 K-ε-GG peptides. To assess and highlight which of the significantly deregulated K-ε-GG peptides were paralleled with opposing effects on total protein expression in the MT/WT case, protein normalized K-ε-GG MT/WT SILAC ratios were multiplied by their corresponding protein level ratio and also by -1 (Supplementary Fig. 2 and Supplmentary Table 1).

The original mass spectra have been deposited in the public proteomics repository MassIVE and are accessible at ftp://MSV000080401@massive.ucsd.edu when providing the dataset password: ubiquitin. If requested, also provide the username: MSV000080401. This data will be made public upon acceptance of the manuscript.

Cell culture, Transfection and Infection

Ishikawa cells were purchased from Sigma, RL-952, 22Rv1, MEF-962, VM-CUB1, NCI-H508 from ATCC, EN from DSMZ, HEC-151 from JCRB. AN3CA, HEC1A, HEC 1B, HEC116, SNG-II, EFE184, KLE were kindly provided by Dr. med. Eleftherios Samartzis and Dr. med. Konstantin Dedes (University Hospital Zurich). Ishikawa, RL-952 and KLE cells were grown in F12/DMEM (Gibco); MEF-962, HEC-151, EN, HEC1A, HEC1B, AN3CA, HEC116 and SNG-II in DMEM (Gibco); 22Rv1 and EFE184 in RPMI medium (Gibco); all were supplemented with 10% FBS (Gibco), 1% Penicilin/Streptomycin/ L-Glutamate. All cells were incubated at 37°C and 5% CO_2. Cells were routinely tested for mycoplasma contamination.

For transient transfection, cells were transfected with either 50 nM *siSPOP* (Hs_SPOP_7, Qiagen), 50 nM *siFOSL1* (Hs_FOSL1_1, Hs_FOSL1_2 and Hs_FOSL1_3, Qiagen) or siControl (Qiagen) using Fugene (Promega). For stable knockdown experiments, cells were infected with pLKO-1 vectors (Sigma) and the following clones were used: *SPOP:* TRCN0000140431 (*shSPOP*); *BRD2*: TRCN00000315433 (*shBRD2_#1*), TRCN0000350530 (*shBRD2_#2*) ; *BRD3:* TRCN0000021376 (*shBRD3_#1*), TRCN0000021377 (*shBRD3_#2*); *BRD4:* TRCN0000021426 (*shBRD4_#1*) TRCN0000021427 (*shBRD4_#2*), and *shBET* (5`-TCCAACTGCTATAAGTACAAT-3`); *CUL-3*: TRCN0000073343 (*shCUL-3_#1*) and TRCN0000073344 (*shCUL-3_#2*); *DEK*: TRCN0000013104 (*shDEK_#1*) and TRCN0000013105 (*shDEK_#2), TRIM24*: TRCN0000021259 (*shTRIM24_#1*) and TRCN0000194983 (*shTRIM24_#2*), *NCOA3*: TRCN0000370320 (*shNCOA3_#1*) and TRCN0000365253 (*shNCOA3_#2*). After infection, cells were selected in the presence of puromycin (2 μg/ml). For over-expression a derivate of the pLX304 vector was used throughout in which the CMV promoter has been exchanged to a PGK promoter and the blastocidin cassette exchanged by mOrange or a puromycin resistance cassette (pLX_TRC_307, available at Addgene as Plasmid 41392, pCW107). All ORFs were cloned into pLX_TRC_307-mOrange using Nhe1 and Mlu1.

Dose response curves and cell growth assay

Cells were seeded (between $1x10^3$and $1x10^4$) in 96-well plate. Cells were consequently treated with serial dilutions of JQ1 or OTX-015 in media for dose response curves or left untreated for cell growth assays. After 96h of treatment in the case of dose response and 6 days for cell growth assays, respectively, cells were washed with PBS and stained with 0.5 % crystal violet solution in 25% methanol. Crystal violet was then solubilized with 10 % Acetic acid and absorbance (OD, 590 nm) was measured in a microplate reader.

Clonogenic assay in methylcellulose

Cells were seeded (between $5x10^3$and $1x10^4$) in methylcellulose (Methocult H4100, StemCell Technologies) in duplicate and treated with vehicle (0.1% DMSO) or drug (JQ1).

Cells were incubated at 37°C and 5% CO_2 for 7-14 days and colonies were stained with MTT solution at 37°C overnight and absorbance (OD, 590 nm) was measured in a microplate reader.

Xenograft Model

All animal experiments were carried out in female athymic nude mice (Balb/c nu/nu, 4–6 weeks old) accordingly to protocol approved by the Swiss Veterinary Authority (No. TI-14-2014). $2x10^6$ Ishikawa and EN cells were resuspended in 200 µl of PBS and subcutaneously injected into the dorsal flank on both sides of nude mice. Once tumors reached approximately 100 mm^3, mice were randomized and intraperitoneally administrated either with vehicle or with JQ1 at 50 mg/kg (twice per day) for indicated time. Tumor growth was recorded using digital caliper and tumor volumes were calculated using the formula $(L \times W^2)/2$, where L=length and W=width of tumor. At the end of the experiment, mice were sacrified, tumors extracted, weighed and histologically analyzed by a board-certified pathologist (J.P.T.) by H&E staining and immunohistochemistry for anti-cleaved Caspase-3 (Cell Signaling protocol).

Antibodies, Immunoblotting, and Immunoprecipiation

Antibodies used in immunoblotting and immunoprecipitation assays were: anti-BRD2 (A302-583A, Bethyl Labs), anti-BRD3 (Sc-81202, Santa Cruz), anti-BRD4 (Sc-48772, Santa Cruz), anti-SPOP (ab81163, Abcam), anti-TRIM24 (Sc-271266, Santa Cruz), anti-NCOA3 (2126, Cell Signaling), anti-DEK (610948, BDBioscience), anti-ERG (Sc-271048, Santa Cruz), anti-FOSL1 (5281, Cell Signaling), anti-VCL (4650, Cell Signaling), anti-ß-actin (4967, Cell Signaling), anti-HA (9658, Sigma), anti-Cleaved Caspase-3 (Asp175) (9661, Cell Signaling). All antibodies were employed at dilutions suggested by the manufacturers.

For immunoblotting, cells were washed with PBS and subsequently lysed in RIPA buffer (Sigma) and sonicated. Protein concentration was determined using the BCA reagent (ThermoFisher), same amounts of protein were separated by SDS-PAGE (Biorad) and transfered onto PVDF membrane (ThermoScientific). The membrane was incubated for one hour in 5% nonfat dry milk/TBS-T blocking buffer followed by incubation with the primary antibody overnight at 4°C. The membrane was washed with TBS-T followed by incubation with horseradish peroxidase-conjugated secondary antibody (Promega).

To detect interactions of SPOP and HA-BRD3, cells were lysed in 1 % NP40 buffer (50mM Tris-HCl pH 7.4, 150 mM NaCl, 1 % NP40) with 2x protease inhibitor cocktail (Complete, Roche), sonicated, and 3 mg of lysate were incubated overnight with 2 µg of anti-HA-tag or control mouse IgG antibody (sc-2025, Santa Cruz Biotechnology) at 4 °C. Subsequently, antibodies were collected by 25 µl protein A/G magnetic beads (88803, Fisher Scientific) for 2h, followed by 2 washing steps with 1 % NP40 buffer. Proteins were eluted by addition of 1x SDS-sample buffer under reducing conditions at 95 °C for 5 min. Quantitative analysis of the Western blots for proteins was normalized to VCL/ACTB expression.

Chemicals

MG-132 and Cycloheximide (CHX) were purchased from Sigma and used at 10 μM and 100 μg/ml in all experiments, respectively. (+) - JQ1 and OTX-015 were purchased from Selleckchem and used at the indicated concentrations.

In Vivo Ubiquitylation Assay

293T cells were transiently transfected with indicated plasmids: pCW107-BRD3-WT or BRD3-Degron-MT (2 μg), pCW107-SPOP-WT or SPOP-MT (2 μg), CMV-8x Ubi-His (2 μg). 42 hours later, cells were treated with MG-132 or DMSO for additional 3 hours. Cells were then washed with PBS and collected by centrifugation. Small amount of cells was lysed in RIPA buffer and the rest in Buffer C (6M guanidine –HCL, 0.1 M Na2HPO4/ NaH2PO4, 10mM Imidazole, pH=8). The whole cells extract was sonicated and incubated with 60 μl of Ni-NTA agarose (Sigma) overnight at 4°C. Next, Ni-NTA beads were washed once with Buffer C, twice with Buffer D (1 volume of Buffer C: 3 volumes of Buffer E) and once with Buffer E (25 mMTris-HCL, 20 mM Imidazole, pH=6.8). Elution of bound proteins was processed by boiling in 1x SDS loading buffer containing 300 mM Imidazole. Samples were loaded, separated by SDS-PAGE, and detected by immunoblotting.

In Vitro Ubiquitylation and Binding assays

Wild-type and SPOP-binding mutant (Degron-MT) constructs of HA-tagged human BRD3 were purified from transiently transfected HEK-293T cells. Wild-type and mutant human SPOP species were cloned, expressed and purified as described previously, using a GST- instead of a MBP-affinity tag7., KLHL9, KLHL13, KLHL21, and Cdc34b were cloned, expressed and purified from *E. coli* as described previously40. CUL3 and RBX1 were purified in a pre-assembled complex from insect cells, and neddylated *in vitro* using purified components as described previously41. *In vitro* ubiquitylation reactions with a total volume of 15 μl were assembled as follows: 107 HA-BRD3-expressing HEK-293T cells were harvested and lysed by sonication in IP buffer (20 mM Tris-Cl pH 7.4, 150 mM NaCl, 5% glycerol, 1 mM TCEP, 1x Roche protease inhibitor cocktail). Immunoprecipitates were prepared with 10 μL of anti-HA affinity gel (Sigma) and washed with IP buffer. For respective samples 2 μl HA-BRD3 IP resin were used and supplemented with 0.3 μM SPOP, KLHL9, KLHL13, or KLHL21, 0.2 μM CUL3-Nedd8/RBX1, 0.7 μM Cdc34, 0.2 μM UbE1 (Boston Biochem) and, 25 μM ubiquitin (BostonBiochem) in ubiquitylation buffer (3 mM ATP, 10 mM $MgCl_2$, 50 mM Tris-Cl pH 7.6, and 0.5 mM DTT). Reactions were incubated at 37°C for 45 minutes and stopped by addition of SDS sample buffer. Samples were separated by SDS-PAGE and visualized through chemiluminescence using using anti-HA (Sigma; A2095), HRP-coupled goat anti-mouse IgG (Biorad; 170-6516), Clarity™ Western ECL Blotting Substrate (Biorad; 1705061) and Fusion FX imaging platform (Vilber Lourmat).

For co-immunoprecipitation experiments *in vitro*, 1 μM recombinant SPOP-WT or mutants and 1 μl of HA-BRD3-WT IP resin were incubated in 200 μl IP buffer (20 mM Tris-Cl pH 7.4, 150 mM NaCl, 5% glycerol) for 1h at 4°C. Thereafter, resin was washed twice in the same buffer and samples were separated by SDS-PAGE and visualized through chemiluminescence using using anti-HA and anti-SPOP (see above).

qRT-PCR

RNA was extracted using the Rnasy kit (Qiagen) and processed by Kapa SybrFAST one-Step qRT-PCR kit according to manufacturer`s instructions. q-PCR was undertaken on an Applied Biosystems StepOnePlus System. The target mRNA expression was quantified using ΔΔCt method and normalized to Cyclophilin expression. The following primers were used: *BRD2*, forward 5`-CTACGTAAGAAACCCCGGAAG-3', reverse 5`-GCTTTTTCTCCAAAGCCAGTT-3'; *BRD3*, forward 5`-CCTCAGGGAGATGCTATC-CA-3', reverse 5`-ATGTCGTGGTAGTCGTGCAG-3'; *BRD4*, forward 5`-CTCCTC-CTAAAAAGACGAAGA-3', reverse 5`-GCCCCTTCTCTTTTTGACTTCGGA-3'; *TRIM24*, forward 5`-CAGCCACAAATGCCTAAGCAG-3', reverse 5`-GTGTTGGGAACTTGGATAACTGG-3'; *SPOP*, forward 5`-GAAATGGTGTTTGCGAGTAAACC-3', reverse 5`-GCCCGAA-CTTCACTCTTTGGA-3'; *FOSL1*, forward 5'-CTGCAGGCGGAGACTGACAA-3' , reverse 5'-TCCGGGATTTTGCAGATGGG-3'; *Cyclophilin*, forward 5'-CAGGTCCTGGCATCTTGTCC -3', reverse 5'-TTGCTGGTCTTGCCATTCCT-3'.

DNA and RNA sequencing of endometrial cell lines

Whole exome sequencing was performed for all endometrial cancer cells line profiled in the Cancer Cell Line Encyclopedia (CCLE)42. This data set was used to determine mutation status for SPOP cell lines included in this study. In addition, RNA sequencing was performed at the Broad Institute using the Illumina TruSeq protocol for 17 CCLE cell lines. Reads were aligned to the human reference genome build hg19 using TopHat version 1.4, and mRNA experssion levels were determined using RNA-SeQC. RPKM values for each cell line were correlated with the median RPKM values of endometrial cancer tissues with recurrent *SPOP* point mutations identified in the TCGA portal6. A threshold of 10 RPKM was used to determine the overlay of robustly expressed genes in the cell lines with the genes expressed in human tumor tissues.

For the analysis of transcriptional output changes in response to SPOP mutants, isogenic Ishikawa cells stably overexpressing either SPOP-WT or SPOP mutants (endometrial-E50K, E47K and prostate-Y87C, W131G) were generated. RNA-sequencing was performed on cells either untreated or treated with JQ1 (500 μM or 2 μM) for 4 hours (Supplementary Table 2). Total RNA was extracted using the Rnasy kit (Qiagen) and sample quality was assessed using Agilent Bioanalyzer. Library preparation (Illumina unstranded True Seq Library incl poly(A)enrichment) and RNA sequencing (Illumina NextSeq high output, v2,1x75bp) was performed by Microsynth. Quality of the sequencing was analysed according to Phred score of Illumina and FastQC (add version). Mapping to Hg38 was pursed by STAR 2.52b. Not expressed genes with counts per million (cpm) <0.5 mapped reads have been filtered. Subsequently, counts were normalized based on the number of reads acquired per sample, transformed in log2 and subjected to voom function of limma package. Signatures were derived comparing samples in Supplmentary Table 2 and the following filters were used to define differentially expressed genes: cpm>45 in at least 2 samples, adjusted p-value<0.05 (according Benjamini-Hochberg test), IIogFCI>0.9.

Human Tumor Samples

We used a previously characterized cohort of primary prostate tumors with annotated *SPOP* mutations by high resolution melt analysis assay followed Sanger sequencing of exon 6 and 73. Due to tissue loss (a common problem encountered with tissue microarrays) only a subset were histologically analyzable. These tumors represent are part of tissue microarrays composed of paraffin-embedded prostate tissue cores from two different institutes of pathology. As previously published, specimens were collected between 1993 and 2007 from the Institute of Surgical Pathology, University of Zurich, Switzerland, and the Institute of Pathology, University of Regensburg, Germany43. The local scientific ethics committees approved both cohorts (approval no.: StV-Nr. 25/2007). Primary endometrial cancer tissues were retrieved from different sources. Tissue sections of 19 tumors culled from the literature with annotated, recurrent *SPOP* mutations were collected as follows: TCGA-D1-A0ZO, TCGA-D1-A167, TCGA-D1-A168, and TCGA-D1-A17D from the Mayo clinic6, TCGA-B5-A0JY, TCGA-B5-A0K0, TCGA-NA-A5I1 from the Duke Cancer Center6, TCGA-BS-A0UT from the University of Hawaii Cancer Center6, TCGA-FI-A2EW from the Washington University6, TCGA-N9-A4Q8, TCGA-DI-A1NN from the MD Anderson Cancer Center6, 2001-02-G049T, 2005-08-G674T, MAD04-00646T, 1090095AT, 1090076AT from the Cooperative Human Tissue Network (CHTN)4, 119, 127, 136 from the Oregon Health & Science University (OHSU)5.

We characterized additional 84 primary endometrial cancer tissues samples by targeted DNA sequencing (36 endometrioid carcinomas, 26 serous carcinomas, 11 clear cell carcinomas, and 11 carcinosarcomas) from two different cohorts from Basel and Zurich44,45,46. Therefore, two 0.6-mm diameter tumor tissue cylinders were punched out of paraffin-embedded tissue blocks and DNA isolated using the Maxwell® 16 FFPE Tissue LEV DNA Purification Kit (Promega) according to the manufacturer's instructions. DNA was quantified using dsDNA HS Assay Kit with Qubit 2.0 (Thermo Fisher Scientific/Life Technologies) and 20 ng were used to prepare libraries using Ion AmpliSeq™ Library Kit 2.0 according to the manufacturer's instructions. A custom panel was applied for PCR-based amplification of *SPOP* gene. Libraries were labeled with the Ion Xpress™ Barcode Adapters 1-96 Kit (Thermo Fisher Scientific/Life Technologies) and quantified by qPCR with the Ion Library Quantitation Kit (Thermo Fisher Scientific/Life Technologies). Twenty to twenty-six libraries were multiplexed for template preparation and enrichment using Ion PI™ Hi-Q™ OT2 200 Kit (Thermo Fisher Scientific/Life Technologies). Enriched samples were then loaded on an Ion PI™ Chip v3 (Thermo Fisher Scientific/Life Technologies) and sequenced on the Ion Proton™ System using Ion PI™ Hi-Q™ Sequencing 200 Kit (Thermo Fisher Scientific/Life Technologies). Sequencing run quality metrics were taken from the Torrent Suite™ Software (Thermo Fisher Scientific/Life Technologies) for each run. Sequencing data was then analyzed with Ion Reporter™ Software (Thermo Fisher Scientific/Life Technologies). We identified another SPOP-D140Y mutated serous cancer, while the remaining cases did not harbor any additional recurrent mutations nor any other type of mutation in *SPOP* at an allelic fraction higher than 0.2. The study was approved by the scientific ethics committee (approval no.: KEK-ZH-NR: 2010-0358).

Immunohistochemistry

For the detection of BET and FOSL1 proteins, slides were first dehydrated. For antigen retrieval, slides were incubated in a waterbath at 98 °C for 20 min using a citrate bufffer at ph 6 (BETs) or ph 9 (FOSL1) (Diapath T0050). For prostate cancer tissue-microarrays, the antigen retrieval for BRD2 and FOSL1 was extended to 40 min in total. Subsequently, slides were cooled to room temperature for 20 min and endogenous peroxidays blocked for additional 10 min with 3 % H_2O_2 (VWR 23615.248). After washing, slides were incubated for 10 min with a protein block solution (Dako X0909). Then, slides were incubated with the primary antibodies at following concentrations: BRD2 (Abcam ab13960; 1:500), BRD3 (Bethyl A302-368A; 1:50), BRD4 (Abcam ab128874; 1:400), and FOSL1 (Sigma Aldrich AV31377; 1:2000) for 1 h in antibody diluent reagent solution (Life Technologies 003118). For prostate cancer tissue-microarrays, the BRD2 antibody was used at a dilution of 1:200. Thereafter, slides were washed and incubated with biotinylated anti-rabbit IgG (Vector BA-1000) in PBS for 30 minuts at room temperature and subsequently washed and incubated another 30 min with Vectastin ABC kit at a dilution of 1:150 in PBS. Detections were performed using the ImmPACT DAB system (Vector SK-4105) for 4 minutes at room temperature followed by nucelar statining with Mayer Hematoxilin (Diapath C0303). Immunohistochemical staining was evaluated as follows for BET proteins: No detectable staining in more than 70% of tumor cell nuclei was referred as negative, 30% or more tumor cell nuclei weakly stained (discernable nucleoli) as weak and more than 30% of nuclei strongly stained (invisible nucleoli) as strong.

Statistical analysis

GraphPad Prism version 7.00 (GraphPad Software) was used for analysis. Data are depicted as means ± SEM unless otherwise specified. An unpaired, two-tailed independent Student's t test with unequal variance assumption was performed to analyze cell culture experiments. Two-way ANOVA (Dunnett’s post test) was used for multiple comparisons. Extra-sum of squares F-test was used to determine statistical significance of dose response curves. The Spearman correlation coefficient was used to compare RNAseq expression data from *SPOP*-mutant human tumors, and BET protein levels with endometrial cell line data. Kendall’s tau-b was used to test correlation of immunohistochemical staining with *SPOP* mutation status.

Supplementary Material

Refer to Web version on PubMed Central for supplementary material.

Acknowledgment

We thank M. Losa, M. Storz, P. Schraml, S. Dettwiler and F. Prutek for help with tissue handling and histology assistance. We thank Q. Zhong for his help with the NGS bioinformatics pipeline. We thank all members of the IRB animal core facility for technical assistance and the animal work. We thank the Oregon Health & Science University (OHSU) and the Cooperative human tissue network (CHTN) for the tissue repository. Also we thank all members of the laboratory for scientific discussions. J.-P.P.T. is funded by a Swiss National Science Foundation Professorship (PP00P3_150645) grant, a Swiss Cancer League (KSL-3654-02-2015) grant, a grant by the Jubiläumsstiftung Swiss Life AG, and a grant by the Vontobel Stiftung. The Swiss National Science Foundation (310030B_160312/1), the European Research Council (268930), SystemsX IPhD (2013/128), Krebsforschungs Schweiz (KFS-3498-08-2014), and a GRL grant from the Korean government fund M.P. This work was also funded in part by a grant to P.J.W. provided by Oncosuisse (KLS-3384-02-2014-R) and the Foundation for Research in Science and the Humanities at the University of Zurich (SWF).

References

1. Roychowdhury S, Chinnaiyan AM. Translating genomics for precision cancer medicine. Annu Rev Genomics Hum Genet. 2014; 15:395–415. DOI: 10.1146/annurev-genom-090413-025552 [PubMed: 25184532]
2. Barbieri CE, et al. Exome sequencing identifies recurrent SPOP, FOXA1 and MED12 mutations in prostate cancer. Nat Genet. 2012; 44:685–689. DOI: 10.1038/ng.2279 [PubMed: 22610119]
3. Blattner M, et al. SPOP mutations in prostate cancer across demographically diverse patient cohorts. Neoplasia. 2014; 16:14–20. [PubMed: 24563616]
4. Le Gallo M, et al. Exome sequencing of serous endometrial tumors identifies recurrent somatic mutations in chromatin-remodeling and ubiquitin ligase complex genes. Nat Genet. 2012; 44:1310–1315. DOI: 10.1038/ng.2455 [PubMed: 23104009]
5. Jones S, et al. Genomic analyses of gynaecologic carcinosarcomas reveal frequent mutations in chromatin remodelling genes. Nat Commun. 2014; 5:5006.doi: 10.1038/ncomms6006 [PubMed: 25233892]
6. Cancer Genome Atlas Research, N. Integrated genomic characterization of endometrial carcinoma. Nature. 2013; 497:67–73. DOI: 10.1038/nature12113 [PubMed: 23636398]
7. Zhuang M, et al. Structures of SPOP-substrate complexes: insights into molecular architectures of BTB-Cul3 ubiquitin ligases. Mol Cell. 2009; 36:39–50. DOI: 10.1016/j.molcel.2009.09.022 [PubMed: 19818708]
8. Theurillat JP, et al. Prostate cancer. Ubiquitylome analysis identifies dysregulation of effector substrates in SPOP-mutant prostate cancer. Science. 2014; 346:85–89. DOI: 10.1126/science.1250255 [PubMed: 25278611]
9. Geng C, et al. Prostate cancer-associated mutations in speckle-type POZ protein (SPOP) regulate steroid receptor coactivator 3 protein turnover. Proc Natl Acad Sci U S A. 2013; 110:6997–7002. DOI: 10.1073/pnas.1304502110 [PubMed: 23559371]
10. Gan W, et al. SPOP Promotes Ubiquitination and Degradation of the ERG Oncoprotein to Suppress Prostate Cancer Progression. Mol Cell. 2015; 59:917–930. DOI: 10.1016/j.molcel.2015.07.026 [PubMed: 26344095]
11. An J, et al. Truncated ERG Oncoproteins from TMPRSS2-ERG Fusions Are Resistant to SPOP-Mediated Proteasome Degradation. Mol Cell. 2015; 59:904–916. DOI: 10.1016/j.molcel.2015.07.025 [PubMed: 26344096]
12. Geng C, et al. Androgen receptor is the key transcriptional mediator of the tumor suppressor SPOP in prostate cancer. Cancer Res. 2014; 74:5631–5643. DOI: 10.1158/0008-5472.CAN-14-0476 [PubMed: 25274033]
13. Nishida M, Kasahara K, Kaneko M, Iwasaki H, Hayashi K. [Establishment of a new human endometrial adenocarcinoma cell line, Ishikawa cells, containing estrogen and progesterone receptors]. Nihon Sanka Fujinka Gakkai Zasshi. 1985; 37:1103–1111. [PubMed: 4031568]
14. Udeshi ND, Mertins P, Svinkina T, Carr SA. Large-scale identification of ubiquitination sites by mass spectrometry. Nat Protoc. 2013; 8:1950–1960. DOI: 10.1038/nprot.2013.120 [PubMed: 24051958]
15. Tsai WW, et al. TRIM24 links a non-canonical histone signature to breast cancer. Nature. 2010; 468:927–932. DOI: 10.1038/nature09542 [PubMed: 21164480]
16. Salmans ML, Zhao F, Andersen B. The estrogen-regulated anterior gradient 2 (AGR2) protein in breast cancer: a potential drug target and biomarker. Breast Cancer Res. 2013; 15:204.doi: 10.1186/bcr3408 [PubMed: 23635006]
17. Groner AC, et al. TRIM24 Is an Oncogenic Transcriptional Activator in Prostate Cancer. Cancer Cell. 2016; doi: 10.1016/j.ccell.2016.04.012
18. Jung M, Gelato KA, Fernandez-Montalvan A, Siegel S, Haendler B. Targeting BET bromodomains for cancer treatment. Epigenomics. 2015; 7:487–501. DOI: 10.2217/epi.14.91 [PubMed: 26077433]
19. Blattner M, et al. SPOP Mutation Drives Prostate Tumorigenesis In Vivo through Coordinate Regulation of PI3K/mTOR and AR Signaling. Cancer Cell. 2017; 31:436–451. DOI: 10.1016/j.ccell.2017.02.004 [PubMed: 28292441]

20. Kwon JE, et al. BTB domain-containing speckle-type POZ protein (SPOP) serves as an adaptor of Daxx for ubiquitination by Cul3-based ubiquitin ligase. J Biol Chem. 2006; 281:12664–12672. DOI: 10.1074/jbc.M600204200 [PubMed: 16524876]
21. Shi J, Vakoc CR. The mechanisms behind the therapeutic activity of BET bromodomain inhibition. Mol Cell. 2014; 54:728–736. DOI: 10.1016/j.molcel.2014.05.016 [PubMed: 24905006]
22. Stonestrom AJ, et al. Functions of BET proteins in erythroid gene expression. Blood. 2015; 125:2825–2834. DOI: 10.1182/blood-2014-10-607309 [PubMed: 25696920]
23. Wang CY, Filippakopoulos P. Beating the odds: BETs in disease. Trends Biochem Sci. 2015; 40:468–479. DOI: 10.1016/j.tibs.2015.06.002 [PubMed: 26145250]
24. Asangani IA, et al. Therapeutic targeting of BET bromodomain proteins in castration-resistant prostate cancer. Nature. 2014; 510:278–282. DOI: 10.1038/nature13229 [PubMed: 24759320]
25. Filippakopoulos P, et al. Selective inhibition of BET bromodomains. Nature. 2010; 468:1067–1073. DOI: 10.1038/nature09504 [PubMed: 20871596]
26. Boi M, et al. The BET Bromodomain Inhibitor OTX015 Affects Pathogenetic Pathways in Preclinical B-cell Tumor Models and Synergizes with Targeted Drugs. Clin Cancer Res. 2015; 21:1628–1638. DOI: 10.1158/1078-0432.CCR-14-1561 [PubMed: 25623213]
27. Shu S, et al. Response and resistance to BET bromodomain inhibitors in triple-negative breast cancer. Nature. 2016; 529:413–417. DOI: 10.1038/nature16508 [PubMed: 26735014]
28. Sahai V, Redig AJ, Collier KA, Eckerdt FD, Munshi HG. Targeting bet bromodomain proteins in solid tumors. Oncotarget. 2016; 7:53997–54009. DOI: 10.18632/oncotarget.9804 [PubMed: 27283767]
29. Lockwood WW, Zejnullahu K, Bradner JE, Varmus H. Sensitivity of human lung adenocarcinoma cell lines to targeted inhibition of BET epigenetic signaling proteins. Proc Natl Acad Sci U S A. 2012; 109:19408–19413. DOI: 10.1073/pnas.1216363109 [PubMed: 23129625]
30. Gibson WJ, et al. The genomic landscape and evolution of endometrial carcinoma progression and abdominopelvic metastasis. Nat Genet. 2016; 48:848–855. DOI: 10.1038/ng.3602 [PubMed: 27348297]
31. Cancer Genome Atlas Research Network. The Molecular Taxonomy of Primary Prostate Cancer. Cell. 2015; 163:1011–1025. Electronic address s. c. m. o. & Cancer Genome Atlas Research, N. DOI: 10.1016/j.cell.2015.10.025 [PubMed: 26544944]
32. Kumar A, et al. Substantial interindividual and limited intraindividual genomic diversity among tumors from men with metastatic prostate cancer. Nat Med. 2016; 22:369–378. DOI: 10.1038/nm.4053 [PubMed: 26928463]
33. Robinson D, et al. Integrative clinical genomics of advanced prostate cancer. Cell. 2015; 161:1215–1228. DOI: 10.1016/j.cell.2015.05.001 [PubMed: 26000489]
34. Theurillat JP, et al. Ubiquitylome analysis identifies dominant-negative deregulation of candidate effector substrates in SPOP-mutant prostate cancer. Science, MS in revision. 2014
35. Kurimchak AM, et al. Resistance to BET Bromodomain Inhibitors Is Mediated by Kinome Reprogramming in Ovarian Cancer. Cell reports. 2016; 16:1273–1286. DOI: 10.1016/j.celrep.2016.06.091 [PubMed: 27452461]
36. Marcotte R, et al. Functional Genomic Landscape of Human Breast Cancer Drivers, Vulnerabilities, and Resistance. Cell. 2016; 164:293–309. DOI: 10.1016/j.cell.2015.11.062 [PubMed: 26771497]
37. Shi X, et al. Loss of TRIM33 causes resistance to BET bromodomain inhibitors through MYC- and TGF-beta-dependent mechanisms. Proc Natl Acad Sci U S A. 2016; 113:E4558–4566. DOI: 10.1073/pnas.1608319113 [PubMed: 27432991]
38. Bendall SC, et al. Prevention of amino acid conversion in SILAC experiments with embryonic stem cells. Mol Cell Proteomics. 2008; 7:1587–1597. DOI: 10.1074/mcp.M800113-MCP200 [PubMed: 18487603]
39. Mertins P, et al. Integrated proteomic analysis of post-translational modifications by serial enrichment. Nat Methods. 2013; 10:634–637. DOI: 10.1038/nmeth.2518 [PubMed: 23749302]
40. Enchev RI, et al. Structural basis for a reciprocal regulation between SCF and CSN. Cell reports. 2012; 2:616–627. DOI: 10.1016/j.celrep.2012.08.019 [PubMed: 22959436]

41. Mosadeghi R, et al. Structural and kinetic analysis of the COP9-Signalosome activation and the cullin-RING ubiquitin ligase deneddylation cycle. Elife. 2016; 5doi: 10.7554/eLife.12102

42. Barretina J, et al. The Cancer Cell Line Encyclopedia enables predictive modelling of anticancer drug sensitivity. Nature. 2012; 483:603–607. DOI: 10.1038/nature11003 [PubMed: 22460905]

43. Mortezavi A, et al. KPNA2 expression is an independent adverse predictor of biochemical recurrence after radical prostatectomy. Clin Cancer Res. 2011; 17:1111–1121. DOI: 10.1158/1078-0432.CCR-10-0081 [PubMed: 21220479]

44. Lebeau A, et al. Oestrogen receptor gene (ESR1) amplification is frequent in endometrial carcinoma and its precursor lesions. J Pathol. 2008; 216:151–157. DOI: 10.1002/path.2405 [PubMed: 18720455]

45. Wild PJ, et al. p53 suppresses type II endometrial carcinomas in mice and governs endometrial tumour aggressiveness in humans. EMBO Mol Med. 2012; 4:808–824. DOI: 10.1002/emmm.201101063 [PubMed: 22678923]

46. Dellas A, Jundt G, Sartorius G, Schneider M, Moch H. Combined PTEN and p27kip1 protein expression patterns are associated with obesity and prognosis in endometrial carcinomas. Clin Cancer Res. 2009; 15:2456–2462. DOI: 10.1158/1078-0432.CCR-08-1732 [PubMed: 19293259]

Europe PMC Funders Author Manuscripts

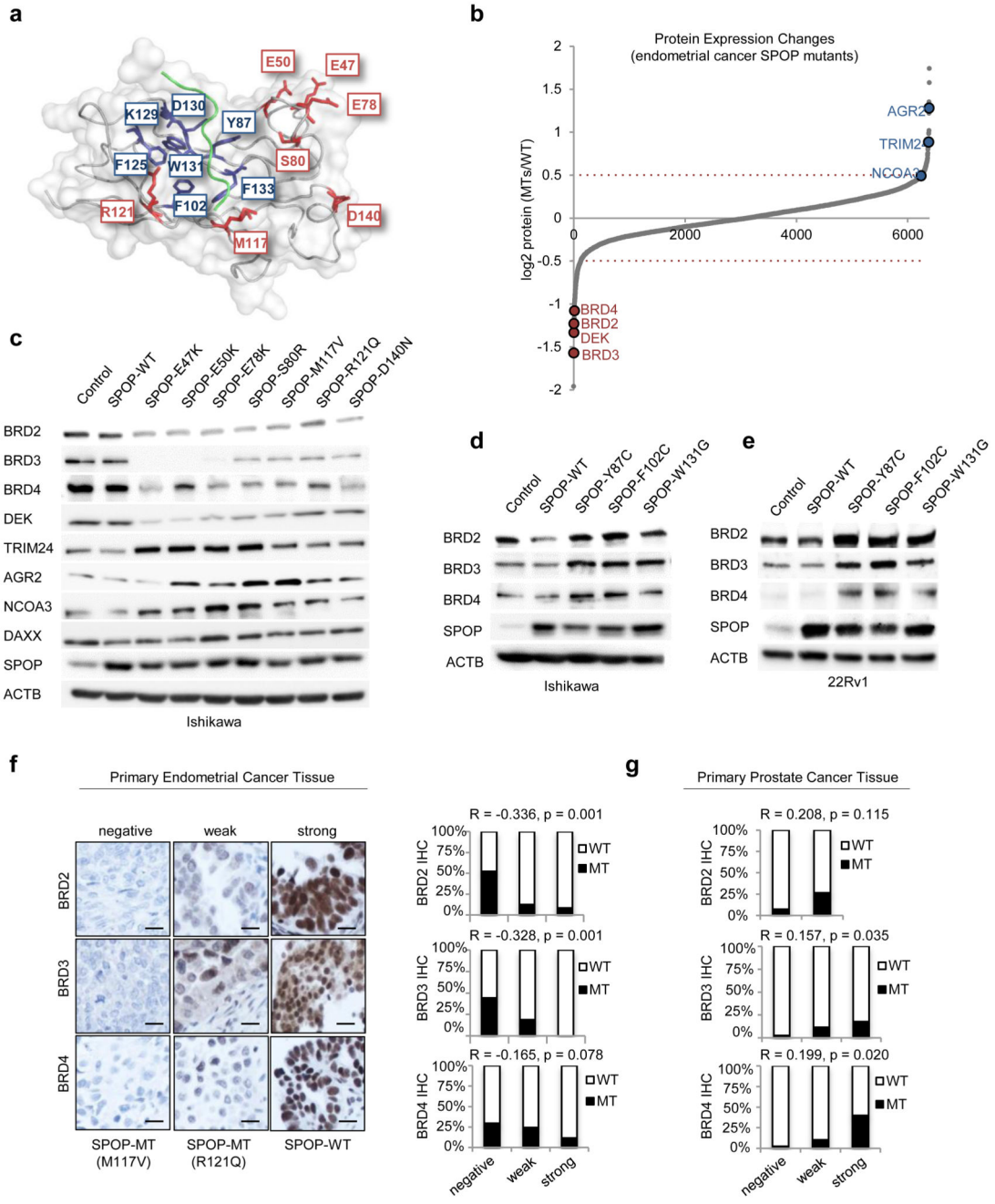

Figure 1. Endometrial and prostate cancer SPOP mutants induce opposing effects on BET protein levels.

(a) Outer surface of the SPOP substrate recognition domain with recurrently mutated amino acid residues highlighted in blue for prostate cancer and red for endometrial cancer, respectively7. Substrate in green in the substrate binding cleft. **(b)** Scatter plot of protein expression changes of SPOP mutants (MTs) vs. SPOP wild type (WT) in Ishikawa endometrial cancer cells, dotted red line = 2 s.d. **(c)** Representative Western blot (WB) validation for indicated proteins in Ishikawa cells stably expressing vector control, SPOP-

Europe PMC Funders Author Manuscripts

Europe PMC Funders Author Manuscripts

WT, or endometrial cancer SPOP-MTs (n=5). **(d)** Representative WB for indicated proteins in Ishikawa endometrial cancer cells expressing prostate cancer SPOP-MTs (n=3). **(e)** Representative WB for indicated proteins in 22Rv1 prostate cancer cells stably expressing prostate cancer SPOP-MTs (n=3). (**f)** Representative images of primary human endometrial cancer tissues stained for BRD2, BRD3 and BRD4 with corresponding expression analysis on primary tumors stratified accordingly SPOP mutation status. Scale bars, 20μm. **(g)** BRD2, BRD3 and BRD4 expression analysis of primary human prostate cancer tissues stratified accordingly *SPOP* mutation status (R correlation coefficient and p values are derived from Kendall's tau-b). N indicates the number of independent experiments performed.

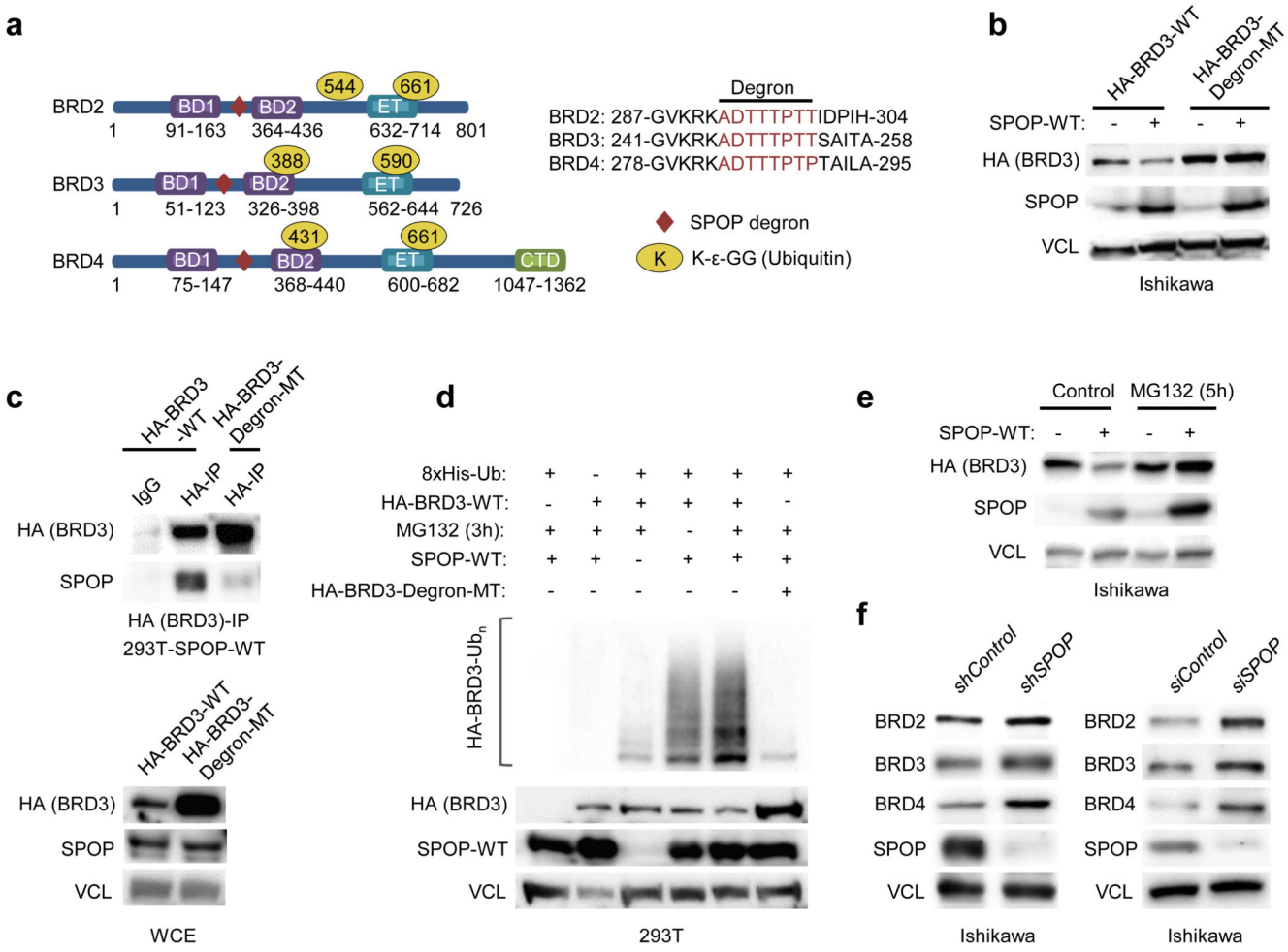

Figure 2. BET proteins are *bona fide* substrates of wild type SPOP.

(a) Schema of BET proteins with bromodomain 1 and 2 (BD1 and BD2), extraterminal (ET) domain, and C-terminal domain (CTD), ubiquitylated lysines (K-ε-GG) detected by mass-spectrometry, and SPOP degron motif. (**b)** Effect of transient SPOP-WT overexpression on protein levels of HA-BRD3-WT and HA-BRD3-Degron-MT assessed by WB in Ishikawa cells (n=3). **(c)** Interaction between SPOP-WT and BRD3-WT or HA-BRD3-Degron-MT. HA-immunoprecipitation (IP) and whole cell extract (WCE) of transiently transfected 293T cells (n=3). **(d)** *In vivo* ubiquitylation of HA-BRD3-WT and HA-BRD3-Degron-MT by SPOP-WT. 293T cells transfected with 8xHis-Ubiquitin (Ub) and indicated constructs followed by MG132 treatment. 8xHis-Ub pull down using nickel beads on lysed cells (n=3). **(e)** HA-BRD3 protein level by WB in Ishikawa cells transiently expressing SPOP-WT and HA-BRD3 with or without MG132 treatment (n=3). **(f)** Representative WB for indicated proteins upon knockdown of *SPOP* with shRNA (left) or siRNA (right) in Ishikawa cells (n=3). Representative WBs are shown. N indicates the number of independent experiments performed.

Europe PMC Funders Author Manuscripts

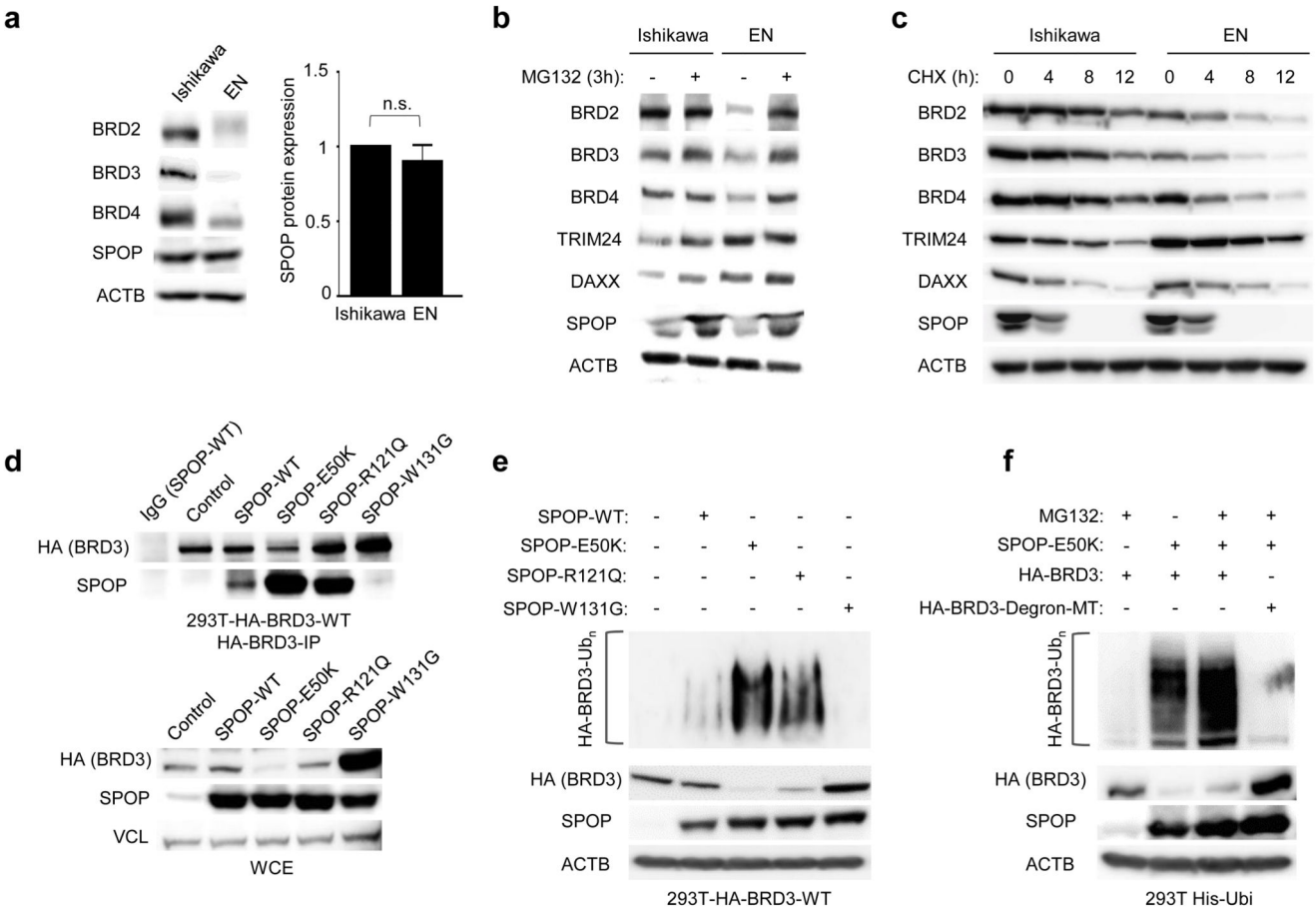

Figure 3. BET proteins are differentially ubiquitylated and degraded by endometrial and prostate SPOP mutants.

(a) Representative WB (n=4) of BET proteins and SPOP in Ishikawa and EN human endometrial cell lines. Statistical significance was determined by unpaired, two-tailed Student's t-test (n.s., non-signicant). **(b)** Representative WB of indicated proteins in Ishikawa and EN cells with or without MG132 treatment (n=3). **(c)** Representative WB of indicated proteins after cycloheximide (CHX) treatment in Ishikawa and EN cells (n=3). **(d)** Interaction between HA-BRD3 and SPOP-WT, endometrial cancer mutants (SPOP-E50K, -R121Q), and one prostate cancer mutant (SPOP-W131G). HA-IP and WCE of transiently transfected 293T cells overexpressing HA-BRD3 and indicated SPOP constructs (n=3). **(e)** Effects of SPOP-WT and SPOP mutants on *in vivo* ubiquitylation of HA-BRD3 (n=3). **(f)** *In vivo* ubiquitylation of HA-BRD3-WT or HA-BRD3-Degron-MT by SPOP-E50K (n=3). Representative WBs are shown. N indicates the number of independent experiments performed.

Europe PMC Funders Author Manuscripts

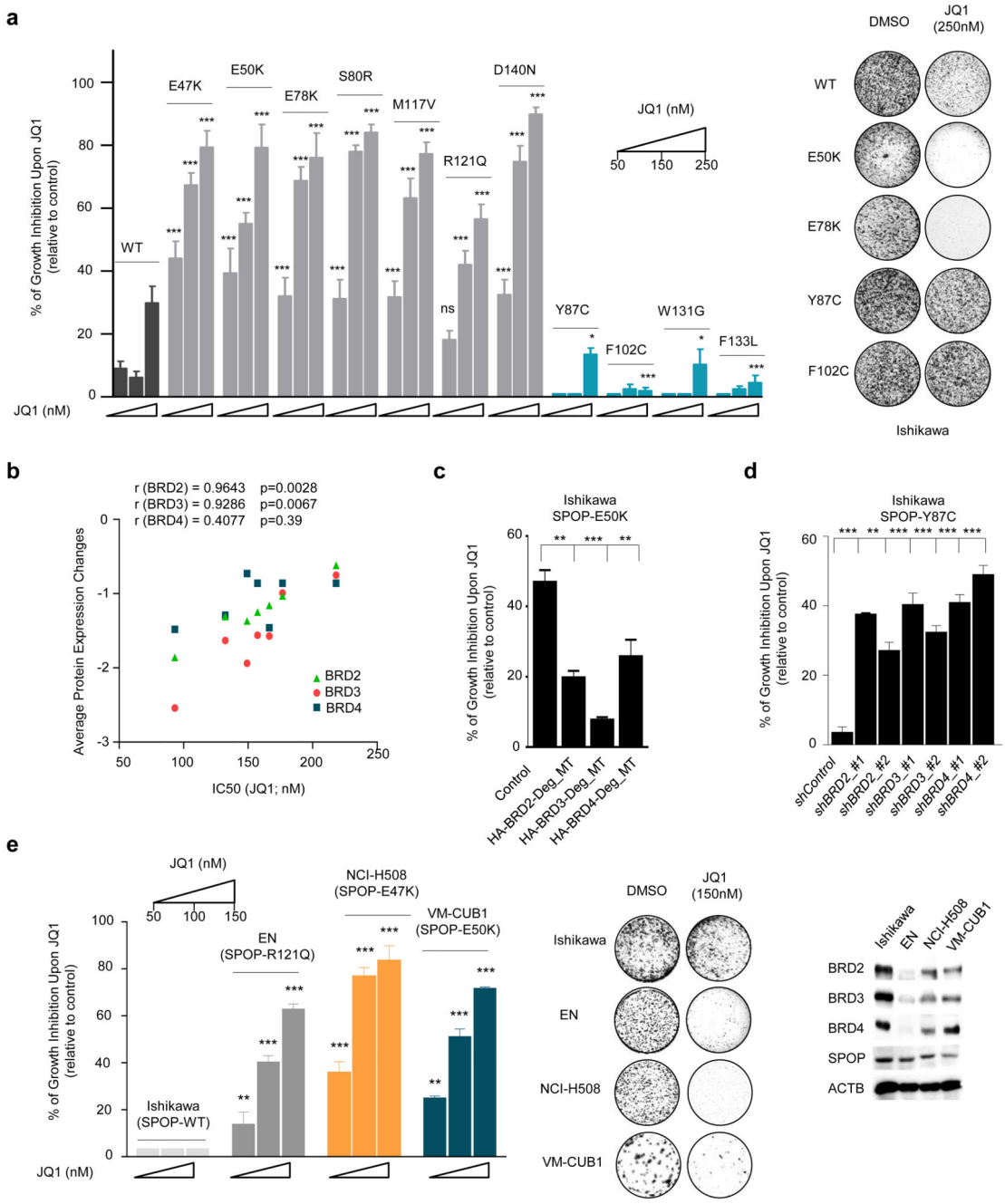

Figure 4. Cancer-type specific SPOP-mutants alter BET inhibitor sensitivity in an opposing manner.

(a) Response to JQ1 in Ishikawa cells stably over-expressing endometrial (E47K, E50K, E78K, S80R, M117V, R121Q, D140N) and prostate cancer (Y87C, F102C, W131G, F133L) SPOP mutants in 3D semi-solid cell culture condition (n=3). P values are indicated above the compared bars (two-way ANOVA with Dunnett's post test, DF= 112 (degrees of freedom)). **(b)** Correlation of IC_{50} (JQ1) shown in Supplementary Fig. 7c with BET protein levels quantified by mass-spectrometry in Ishikawa cells stably expressing recurrent

Europe PMC Funders Author Manuscripts

endometrial SPOP-MTs (r- and p value Spearman rank correlation). **(c)** Response to JQ1 (250nM) of Ishikawa cells stably overexpressing SPOP-E50K and different BET protein degron mutant constructs (Degron MT) (n=3). **(d)** Effect of single shRNA-mediated depletion of *BRD2*, *BRD3* and *BRD4* on JQ1 (200nM) sensitivity in Ishikawa-SPOP-Y87C cells (n=3). **(e)** JQ1 sensitivity of SPOP-WT Ishikawa, SPOP-R121Q-mutant EN human endometrial cancer cell lines; SPOP-E47K-mutant NCI-H508 human large intestine cancer cell line and SPOP-E50K-mutant VM-CUB1 human urothelial cancer cell line in 3D semi-solid culture (n=4). P values are indicated above the compared bars (two-way ANOVA with Dunnett's post test, DF= 30). N indicates the number of independent experiments performed. All error bars, mean ± SEM. Statistical significance was determined by unpaired, two-tailed Student's t-test unless otherwise specified (*P < 0.05, **P < 0.01, ***P < 0.001).

Europe PMC Funders Author Manuscripts

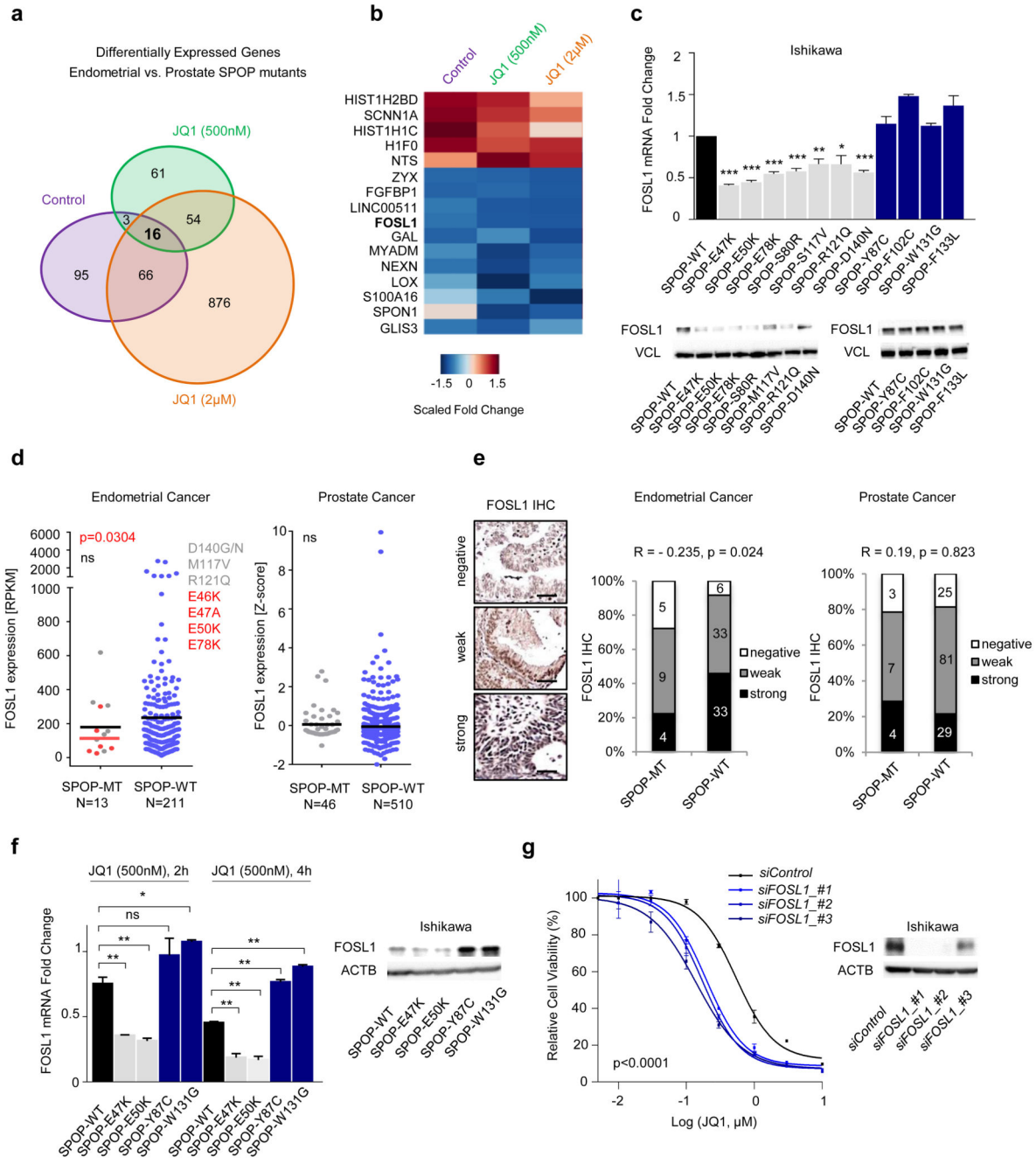

Figure 5. Downregulation of *FOSL1* sensitizes to JQ1 treatment.

(a) Venn diagram depicting the overlap of significantly differentially expressed genes in Ishikawa cells stably expressing either endometrial (E47K, E50K) or prostate (Y87C, W131G) cancer SPOP MTs without or with JQ1. Overlay is significant p value < 0.05 (Benjamini-Hochberg test). **(b)** Heat map showing the fold change of the 16 genes included in the intersection of panel a. **(c)** FOSL1 mRNA (normalized to *Cyclophilin*) and protein levels of Ishikawa cells stably expressing SPOP-WT and either endometrial or prostate cancer SPOP MTs (n=4). **(d)** *FOSL1* mRNA expression in endometrial30 and prostate31–33

Europe PMC Funders Author Manuscripts

Europe PMC Funders Author Manuscripts

cancer patient datasets stratified accordingly to *SPOP* status. P value was derived from an unpaired t-test with Welch's correction. **(e)** Representative images of human primary endometrial cancer tissues stained for FOSL1 with corresponding expression analysis on human primary tumors stratified accordingly to *SPOP* mutation status (p value Kendall's tau-b). Scale bars, 80μm. **(f)** FOSL1 mRNA and protein expression levels after JQ1 (500nM) treatment in Ishikawa cells stably expressing SPOP-WT and either two endometrial (E47K, E50K) or two prostate (Y87C, W131G) cancer SPOP MTs (n=3)**. (g)** Dose-response curves to JQ1 of Ishikawa-SPOP-Y87C cells upon *FOSL1* knockdown (n=3). P value is indicated below the dose-response curves by extra-sum of squares F test. Corresponding WB validation of *FOSL1* knockdown. N indicates the number of independent experiments performed. All error bars, mean ± SEM. Statistical significance was determined by unpaired, two-tailed Student's t-test unless otherwise specified (n.s., non-signicant, *P < 0.05, **P < 0.01, ***P < 0.001).

Europe PMC Funders Author Manuscripts

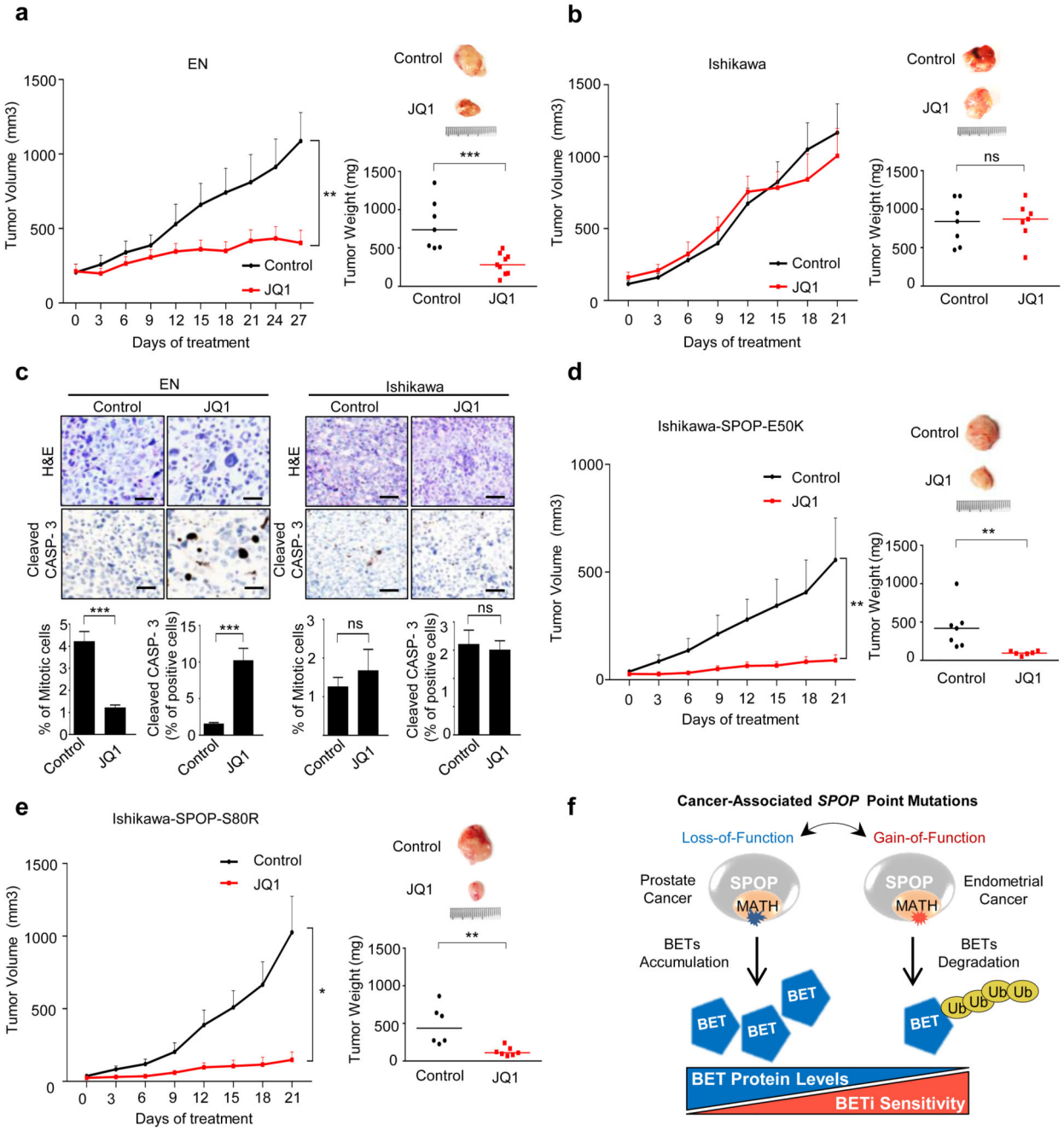

Figure 6. Endometrial SPOP mutants sensitize to JQ1 treatment *in vivo*.

(a) Tumor growth kinetics and graph showing the individual tumor weight with (n=9) or without (n=7) JQ1 in xenografts established from EN. **(b)** Tumor growth kinetics and graph showing the individual tumor weight with (n=7) or without (n=7) JQ1 in xenografts established from Ishikawa. **(c)** Representative histology and quantification of mitotic and apoptotic cells in EN and Ishikawa xenografts treated either with vehicle or JQ1. **(d)** Tumor growth kinetics and graph showing the individual tumor weight with (n=7) or without (n=6) JQ1 in xenografts established from Ishikawa stably over-expressing SPOP-E50K. **(e)** Tumor

growth kinetics and graph showing the individual tumor weight with (n=6) or without (n=7) JQ1 treatment in xenografts established from Ishikawa stably over-expressing SPOP-S80R. Representative images of tumors for each xenograft group are shown. Mean tumor volume + SEM is shown. Statistical significance was determined by unpaired, two-tailed Student's t-test (*P < 0.05, **P < 0.01, ***P < 0.001). **(f)** Model showing the differential effect of cancer-specific SPOP mutations on both BET protein levels and sensitivity to BET inhibitors.

Europe PMC Funders Author Manuscripts